

Compression of the current sheet and its impact into the reconnection rate

S. I. Vainshtein¹, Z. Mikić², R. Sagdeev³

¹*University of Chicago*

²*Science Applications International Corporation (SAIC)*

³*University of Maryland*

Abstract

Numerical simulations of strongly compressible MHD corresponding to a stellar atmosphere with substantial gravity and near force-free magnetic fields show that the current sheet collapses (its width decreasing substantially). As a result, the reconnection rate increases dramatically.

I. INTRODUCTION

It is well known that magnetic configurations are dissipating rather slowly in astrophysical conditions. Obviously, the Ohmic reconnection time,

$$t_O = \frac{L^2}{\eta},$$

where L is the characteristic magnetic scale, and η is resistivity, is huge, comparable with cosmological times.

The dissipation becomes much more efficient in the presence of current sheets. In particular, the Sweet-Parker (SP) flow in the vicinity of the current sheet results in faster reconnection rate, so that it can be estimated as

$$t_{SP} = \frac{t_O}{S^{1/2}} = t_A S^{1/2}, \quad (1)$$

where S is Lundquist number,

$$S = \frac{C_A L}{\eta},$$

C_A is Alfvén velocity,

$$C_A = \frac{B}{\sqrt{4\pi\rho}},$$

and t_A is Alfvén time,

$$t_A = \frac{L}{C_A}, \quad (2)$$

see [1], [2]. As $S \gg 1$ in astrophysical conditions, the SP mechanism (1) provides magnetic dissipation which is much faster than Ohmic. Still, this mechanism is rather slow compared with the time of stormy events like solar flares, or flares in the stars.

More efficient mechanism was suggested by Petschek [3], with reconnection time,

$$t_P = t_A \frac{8 \ln S}{\pi}.$$

The Alfvén time (2) is usually small enough, so that the characteristic time of stormy and violent events is comparable or even slightly larger than it. For this reason, the time t_P is sufficient to explain these stormy events. It was pointed out however, that there should be some additional nontrivial conditions satisfied in order this mechanism to work. In

particular, there are difficulties for this mechanism in simple two-dimensional geometry, without additional effects like anomalous resistivity, Hall currents, localized resistivity etc., see e.g. [4], [5], [6], [7].

II. IMPACT OF THE COMPRESSIBILITY.

Most of the numerical simulations and analysis are provided by incompressible or only slightly compressible situations, although it was suggested long ago that compressibility may speed up the reconnection rate, [9]. It was indeed shown experimentally that the compression plays significant role in the reconnection process, [10].

Previous quite extensive numerical simulations [8] persistently showed that force-free compressible reconnection rate increases dramatically. These simulations also confirm that compressibility plays key role in the reconnection process. In particular, it was noticed that the current sheet is strongly compressed, or one may say that it collapses, increasing the density. As a result of compression, the sheet width shrinks, leading to increased reconnection rate.

The compression is substantial in the low density plasmas, typical for force-free (or near force-free) solar and stellar atmospheres, where the forces are balanced not by a regular pressure, but rather by magnetic pressure.

The plasma and current sheet collapse is in fact forming a singularity, suggested by B.C. Low, [11]. That was strictly one-dimensional model, and in fact, in the vicinity of the current sheet the magnetic configuration is indeed quasi-one-dimensional.

The simplest way to see the plasma compression is to consider an one-dimensional model, where all the quantities depend on x only, and magnetic field $\mathbf{B} = \{0, B_y(x, t), B_z(x, t)\}$. The force-free equilibrium can be sustained if

$$B_y^2 + B_z^2 = \text{const.} \quad (3)$$

We suggest that B_y is an odd function of x , changing sign at $x = 0$, then B_z is an even function, and (if $B_z \geq 0$) with maximum at the origin. Suppose that the characteristic length of B_y is δ , then, according to (3), the characteristic scale of B_z would be the same.

Assuming that δ is "small" (we will define this scale later), we conclude that B_z has a sharp maximum at the origin.

The equation of B_z evolution is as follows,

$$\partial_t B_z + \nabla \cdot \mathbf{v} B_z = \eta \nabla^2 B_z \quad (4)$$

The velocity consists in fact of only one component, v_x , and, as seen from (4), it is an odd function vanishing at the origin. Consider then (4) at $x = 0$. If we look for stationary solutions, $\partial_t = 0$, and, as $v_x(x = 0) = 0$, we get,

$$B_z(x = 0) \nabla \cdot \mathbf{v} = \eta \partial_x^2 B_z \quad (5)$$

As the right-hand-side is negative (corresponding to the maximum), we conclude that $\nabla \cdot \mathbf{v} < 0$, i.e., compression. We now suppose that δ correspond to the width of the SP current sheet,

$$\delta = \delta_{SP} = \frac{L}{S^{1/2}}. \quad (6)$$

Then, for not very strong B_z , corresponding to the compressible media, we have,

$$\nabla \cdot \mathbf{v} \approx -\frac{\eta}{\delta^2} = -\frac{1}{t_A}. \quad (7)$$

It follows from (7), that, in case of SP current sheet, the compression proceeds with the fastest time in the problem.

The meaning of this compression is as follows. As mentioned above, the equilibrium (3) can be sustained if magnetic pressure $B_z^2/(8\pi)$ has a sharp maximum at the origin compensating magnetic "wall" consisting of sharp increasing of B_y^2 . Without this maximum of B_z the configuration would collapse to the $x = 0$ point (due to the $B_y^2/(8\pi)$ pressure). However, finite diffusivity smoothies out this maximum, not allowing the equilibrium (3) to survive. This plasma collapse tries to involve magnetic field due to the frozen-in conditions, thus resulting in magnetic collapse as well. It is this situation that was observed in previous simulations and also will be reported below.

III. THE ROLE OF THE GRAVITY

Theoretically, we can consider force-free fields (of stellar coronas), completely neglecting the pressure, as in [11]. In that case, the compressible part of the Lorenz forces are balanced

by magnetic pressure. In fact, any compression in plasma should increase the magnetic pressure gradient to balance and eventually to stop the compression. However, previous numerical simulations persistently showed that magnetic pressure is not sufficient, and that the regular pressure grows. As follows from Sec. II, the magnetic pressure $B_z^2/(8\pi)$ is unable to balance all the forces because of the finite diffusivity, quite substantial in SP current sheets.

In spite of the growing regular pressure, we did not seem to find anything dramatic in its impact. The reconnection is still much faster than in SP current sheets. In particular, it follows from (1) that the reconnection rate for SP flows is

$$r_{SP} = \frac{1}{t_{SP}} \sim \eta^{1/2}, \quad (8)$$

and, as η is low for astrophysical conditions (in dimensionless units), the reconnection is inefficient. In previous simulations, with pressure included, the reconnection rate $r \sim \eta^{0.2 \div 0.3}$, i.e., much faster than the SP rate.

Still, the pressure seems to somewhat slow down the reconnection. We note, that dramatic increase of density perturbation, and therefore increase of the pressure, is unlikely in the stellar atmospheres. Indeed, unless there are special conditions (satisfied, e.g., for the solar prominences), in the presence of gravity forces, the density “blobs” cannot be sustained in coronas for a long time, and they are supposed to slip down along the magnetic field lines.

We expect that, if the fall down time is much less than the Alfvén time, then, roughly speaking, the matter remains in stratified and almost unperturbed state all the time during the reconnection process.

We introduce a dimensionless number,

$$Z = \frac{gL}{C_A^2 \beta^{1/2}} = \frac{gL}{C_{As}}, \quad (9)$$

where g gravity acceleration,

$$\beta = \frac{p}{B^2/(8\pi)} \sim \frac{s^2}{C_A^2},$$

and s is the sound speed. Note that we consider low pressure case, i.e., $\beta \ll 1$.

In equilibrium state, the matter is stratified along the field lines. We suppose that the pressure is constant on the photosphere, and therefore, in gravitational equilibrium, this

stratification is independent of field line position, i.e., the density and pressure are functions only of vertical dimension. In other words, in equilibrium state, the forces

$$\mathbf{g}\rho - \nabla p + \frac{\nabla \times \mathbf{B} \times \mathbf{B}}{4\pi} \quad (10)$$

are balanced separately, i.e., there is hydrostatic equilibrium of a stratified media,

$$\mathbf{g}\rho - \nabla p = 0, \quad (11)$$

and magnetic equilibrium, i.e., force-free field,

$$\nabla \times \mathbf{B} \times \mathbf{B} = 0.$$

These two equilibrium's have two different time-scales to establish. We will look for the case when the first equilibrium has a shorter time-scale, and therefore established, while the magnetic field is evolving slower.

The estimated scale-height of the stratified media (11) is

$$H = \frac{s^2}{g}, \quad (12)$$

We will suppose that

$$Z > \beta^{1/2}, \quad (13)$$

a condition, easily satisfied in the stellar atmospheres (like the sun). Then,

$$H < L. \quad (14)$$

Then, the recovery time for any density perturbation to vanish and to return to the stratification (11) would be just the falling time on one scale-height (12),

$$t_f = \sqrt{\frac{2H}{g}} = \frac{\sqrt{2}s}{g}. \quad (15)$$

Obviously, we are interested in the case of fast established stratification, that is,

$$t_f \ll t_A, \quad (16)$$

which is equivalent to the requirement

$$Z \gg 1, \quad (17)$$

an inequality stronger than (13).

In this paper we are dealing only with the limiting case (17), leaving more general case for the future studies. Presenting density and pressure as

$$\rho = \rho_0 + \delta\rho,$$

$$p = p_0 + \delta p.$$

Thus, in the zeroth approximation, the first two terms in (10) cancel each other,

$$\mathbf{g}\rho_0 - \nabla p_0 = 0,$$

cf. (11). Assuming that (16), or (17) is satisfied, the density perturbation vanishes for a short time t_f , being generated for a much longer time t_A , according to (7). Therefore the density perturbation is weak,

$$\frac{\delta\rho}{\rho_0} = \frac{t_f}{t_A} = \frac{1}{Z} \ll 1, \quad (18)$$

In the first approximation, the gravitational force is no longer balanced by the gradient of the pressure, although they are of the same order of magnitude. Both terms can be estimated as

$$g\delta\rho \approx g\frac{\rho_0}{Z},$$

while the estimation of the Lorentz force is

$$\rho_0 \frac{C_A^2}{L}.$$

Then, the ratio of the first two terms in (10) to the Lorentz force is

$$\frac{gL}{ZC_A^2} = \frac{s}{C_A} = \beta^{1/2} \ll 1.$$

Summarizing: In the zeroth approximation, the first two terms in (10) are canceling each other, and in the first approximation they are small compared to the Lorentz force, if $Z \gg 1$. We will consider the momentum equation in this approximation. As the buildup of the density and therefore of the pressure, according to (18), is weak, we do not expect the pressure to impede the reconnection process, as opposed to our previous simulations.

IV. FORMULATION OF THE PROBLEM

The problem is solved in two-dimensional (compressible) MHD. That means that all quantities depend on x, y only (and independent of z), but the fields contain all three components (the so-called 2.5-dimensional MHD). Thus,

$$\mathbf{B} = \{\mathbf{B}_\perp(x, y, t), B_z(x, y, t)\} = \{\partial_y A_z(x, y, t), -\partial_x A_z(x, y, t), B_z(x, y, t)\}. \quad (19)$$

The initial configuration is depicted in Fig. 1. The magnetic field is rooted on the photosphere, $y = 0$, decreasing dramatically up into the corona. The density is stratified, i.e., it is decreasing (exponentially) from the photosphere into the corona. The configuration is considered to be periodic in horizontal direction (i.e., in X -direction). We are solving the induction equation,

$$\partial_t \mathbf{B} = \nabla \times [\mathbf{v} \times \mathbf{B}] + \eta \nabla^2 \mathbf{B}, \quad (20)$$

with zeroth initial velocity \mathbf{v} . The momentum equation is presented by Navier-Stokes equation with forcing as in (10), in approximation of $Z \gg 1$, see Sec. III.

We can imagine that two “sunspots” of opposite polarities are initially far away of each other, and therefore they are not connected. Suppose that, in the course of evolution, they approach each other, forming a configuration similar to that depicted in Fig. 1. Due to frozen-in conditions, the topology of the field lines is not easy to change, and, for a while, they remain disconnected from each other. Due to finite conductivity, a current sheet will form, and the reconnection starts. Further evolution is observed in our numerical simulations.

The case of $B_z = 0$ corresponds to current free equilibrium. That means that, if the pressure is neglected (which is justified in low- β plasma (of stellar atmospheres), the only equilibrium to which the configuration is tending to settle down is current-free. Obviously, the configuration depicted in Fig. 1, does not correspond to this equilibrium, and it has to form a current sheet, the situation described by Syrovatsky, [12]. If $B_z \neq 0$, smooth distributed currents (not current sheets) may be formed in corona, so that the configuration may settle down to force-free equilibrium with (smooth) currents in the corona. This situation is much less understood, being actually typical for stellar atmospheres, and therefore is interesting for numerical studies.

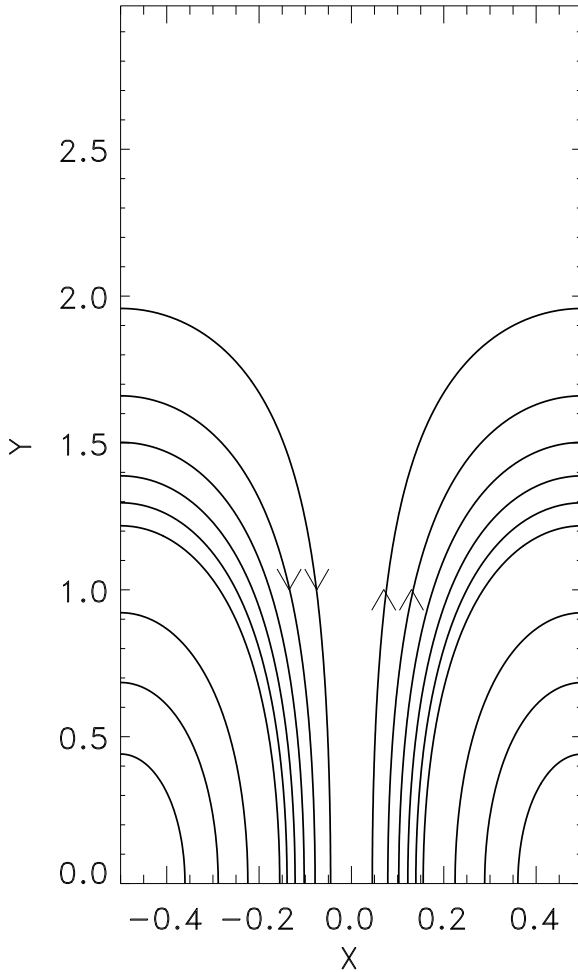


FIG. 1: Initial configuration

The Alfvén velocity, is small on the photosphere, and it reaches a maximum in the middle corona, and again very small (numerically zero) is in the upper corona. For this reason, almost nothing happens on the photospheric level, where the Alfvén velocity is 100 times less than its maximum, and, for the same reason, practically everything is still well above in corona. The reconnection is expected to take place where the Alfvén speed is maximal, and it is indeed observed in the vicinity of its maximum.

Naturally, we have in mind a real three-dimensional configuration that can be approximated as a two-dimensional. That means that the field in ignorable direction z is eventually

also closing at the photosphere. In self-consistent approach, we may assume that the normal component of the velocity vanishes on the photosphere, which means, in particular, that $v_z = 0$.

The configuration depicted in Fig. 1, or other similar configurations with slightly different geometry, were treated in several (at least three) different codes, with quantitatively similar results, described in the tho next sections.

V. RESULTS OF NUMERICAL SIMULATIONS: MEASUREMENTS OF THE FIELD EVOLUTION

Previous studies were devoted to the so-called rosette-structure, in which case the current sheet formation is inevitable, see [13]. It has been shown that the reconnection rate strongly increases, as compared with the SP rate, [8], see also the main results in Fig. 8. All previous simulations are dealing with no gravity, $Z = 0$, see definition in (9). The new simulations are devoted to the opposite limiting case, $Z \gg 1$, and they are performed with pseudo-spectral code.

A. Dramatic magnetic field reconstruction

The main evolution of the magnetic field is described by the behavior of the vector-potential, defined in (19). According to (20), the governing equation for it reads,

$$\partial_t A_z + \mathbf{v} \nabla A_z = \eta \nabla^2 A_z, \quad (21)$$

which is equivalent to the z -component of the Ohm's law,

$$\mathbf{E} + \mathbf{v} \times \mathbf{B} = \eta \mathbf{j}, \quad (22)$$

where

$$\partial_t A_z = -E_z. \quad (23)$$

In astrophysical conditions, dimensionless value of $\eta \ll 1$, and therefore the right-hand-side in (22), is negligible, that is, in fact, the electric field is defined from

$$\mathbf{E} + \mathbf{v} \times \mathbf{B} = 0, \quad (24)$$

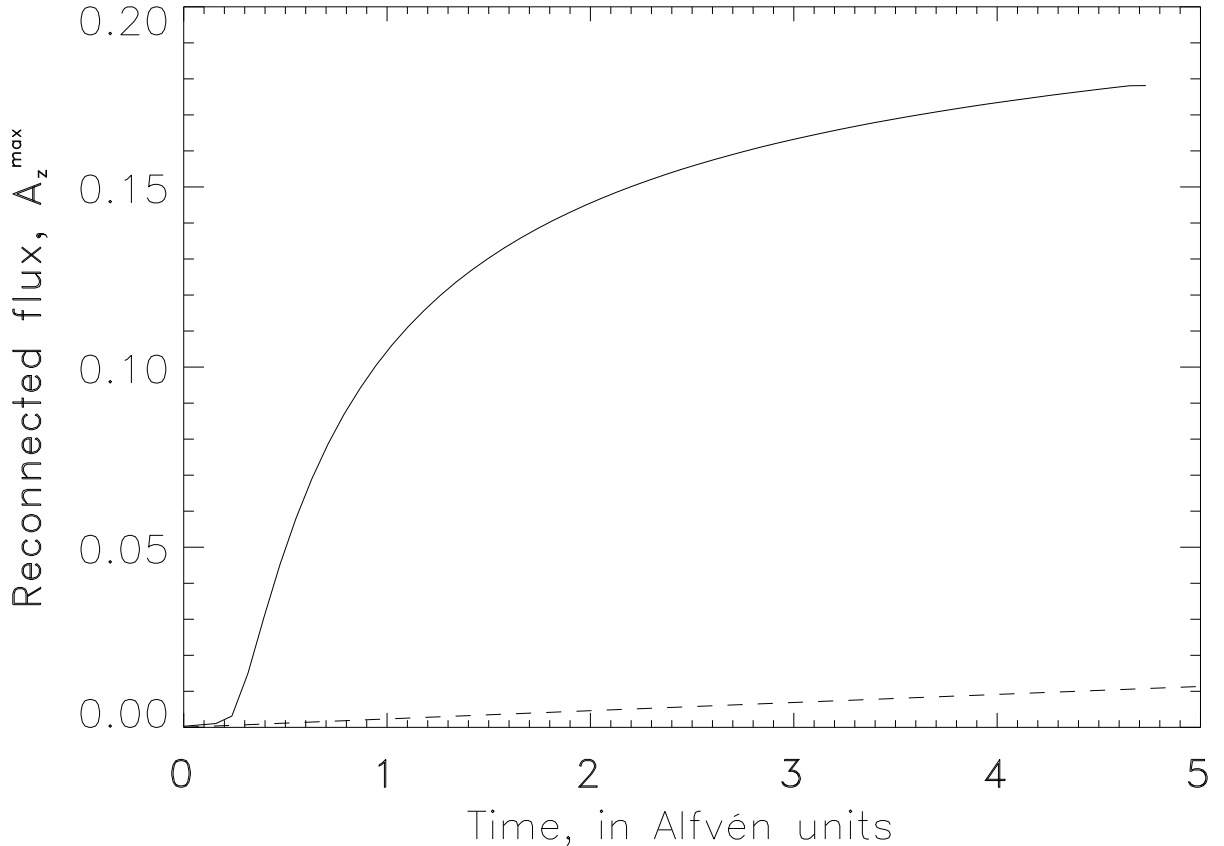


FIG. 2: The reconnection flux versus time; $\eta = 0.00125$, for fully nonlinear case from numerical simulations (solid line), and for pure Ohmic decay (dashed line).

which corresponds to the frozen-in conditions. This is true everywhere except at the x -point where $B_x = B_y = 0$. Here, the typical electric field is weak, and, as seen from (22), is defined only by finite (and very weak) Ohmic decay.

The situation is dramatically different in the presence of strong currents, – current sheets, which appear in the vicinity of the x -points. It is in these places where the reconnection occurs. In our case, the x -point occurs somewhere on the Y -axis, possibly moving up and down along the axis in the middle corona.

In initial configuration, Fig. 1, $A_z(x = 0, y) \equiv 0$ on the Y -axis. Afterwards the reconnection occurs, and A_z grows on the axis. Almost nothing occurs both on the photosphere, at

$y = 0$, and high in the corona, where the Alfvén velocity is small. As a result, $A_z(x = 0, y)$ acquires a maximum corresponding to the x -point (where $B_x = B_y = 0$). The value of the maximum, A_z^{\max} , characterizes the reconnected flux. It is important to estimate, how fast is this maximum growing, that is, how much flux is reconnected during a fixed amount of time. In fact, the time derivative of A_z in this point, according to (23), defines the electric field (responsible for the particle acceleration to high energies, etc.). In some runs, the maximum of electric field may present the efficiency of the reconnection process. However, this happens only if this maximum is not sharp, i.e., it is surrounded by high values of electric field - in the vicinity of the maximum. Otherwise, the maximum is short-lived. That means that relatively fast reconnection did happen, but only for a short time, so that only a small fraction of magnetic flux reconnected. For this reason, we will calculate average electric field, which is compared with maximum possible electric field,

$$E^{\max} = C_A B_{\perp}, \quad (25)$$

see (24), where the velocity was replaced by Alfvén velocity, maximal in this problem.

Figure 2 illustrates one of the runs of our simulations. It can be seen that, for only several Alfvén times, a substantial amount of magnetic flux is reconnected. This is compared with pure Ohmic decay, when all nonlinear effects are switched off. Note that Ohmic decay (with superconductive boundary condition at the bottom and zero at the top, and periodic conditions on the left and right), also results in reconnection, but very slow, as seen from the figure.

The final state of magnetic field is depicted in Fig. 3, which should be compared with initial, Fig. 1. It can be seen that much of the flux has been reconnected. Note that, if all the nonlinear effects are switched off, that is, only Ohmic decay remains, then, the configuration at the same moment of time would be practically the same as initial depicted in Fig. 1.

The magnetic energy is decreasing quite efficiently during the evolution, see Fig. 4. It is clear that the corresponding energy drop during the same time in linear case, that is, only due to pure Ohmic decay, is much less efficient. The energy at $t = 5$, corresponding to the configuration in Fig. 3, proved to be close to the theoretical final energy, as seen from the

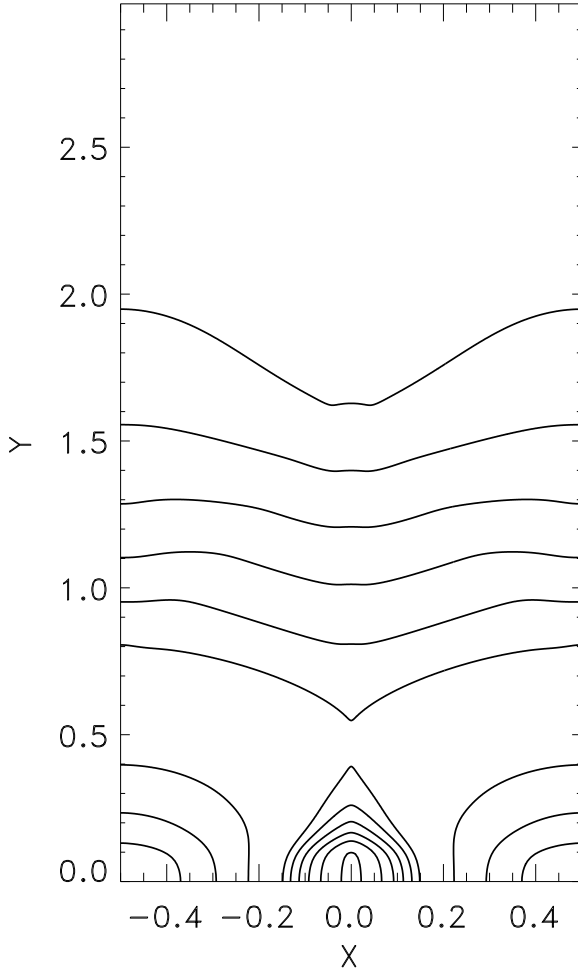


FIG. 3: Final configuration, after reconnection; $t = 5$ and $\eta = 0.00125$

Fig. 4 (dashed-dotted line).

B. Strong currents

Initial magnetic field is not at equilibrium, and, of course, the system is trying to reach equilibrium state. This can be achieved either by current-free configuration, for small or absent B_z , or force-free state, – for finite B_z . However, the initial topology of the field lines is incompatible with final equilibrium state, see [12], and therefore the field lines should

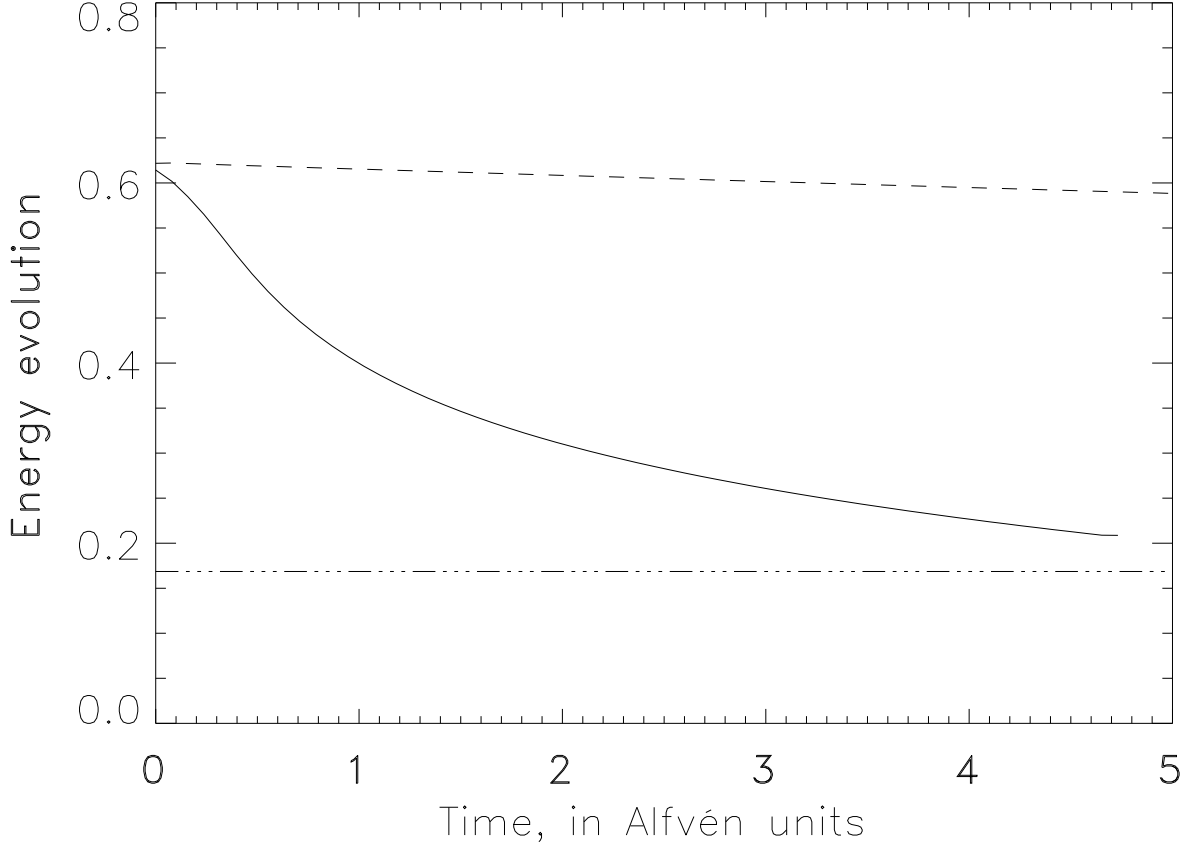


FIG. 4: Evolution of magnetic energy, for $\eta = 0.00125$, $Z \gg 1$, depicted with a solid line. This is compared with pure Ohmic decay (dashed line), which would eventually end up in the lower state depicted with dashed-dotted line.

reconnect. As the system is driven to equilibrium by Lorentz forces, the reconnection should be faster than Ohmic. This can be achieved if strong currents are generated, i.e., in fact current sheets.

As seen from Fig. 5, strong currents are indeed formed. An equilibrium state would be presented by smooth currents, like the initial in the figure, but this state is achieved only after part of the flux is reconnected, and this process of reconnection is accompanied by strong currents.

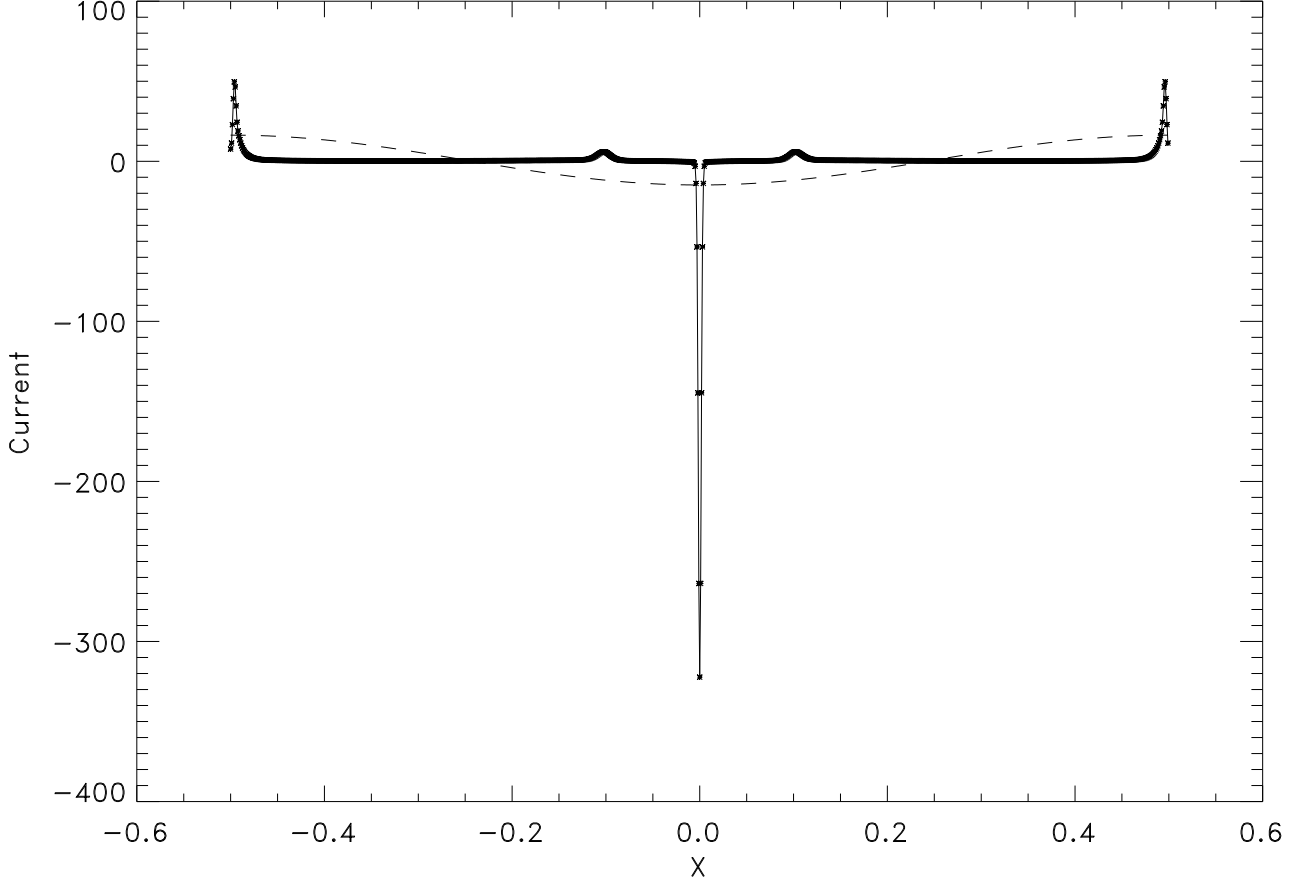


FIG. 5: Section of currents at x -point at $t = 1$, $\eta = 0.00125$, solid line with asterisks. It is compared with initial current – smooth dashed line.

C. Strong compression

As mentioned above, the equilibrium state can be achieved only after some flux is reconnected. Thus, the current sheet is inevitably formed. Of course, the starting width of the sheet is defined by SP mechanism, see (6). In the vicinity of the sheet the configuration is in quasi-one-dimensional equilibrium (3). As mentioned in Sec. II, B_z -component acquires maximum at the center of the sheet. For this, there should be some compression, that is, B_z -component should increase approximately in

$$\frac{B_{\perp}}{B_z} \quad (26)$$

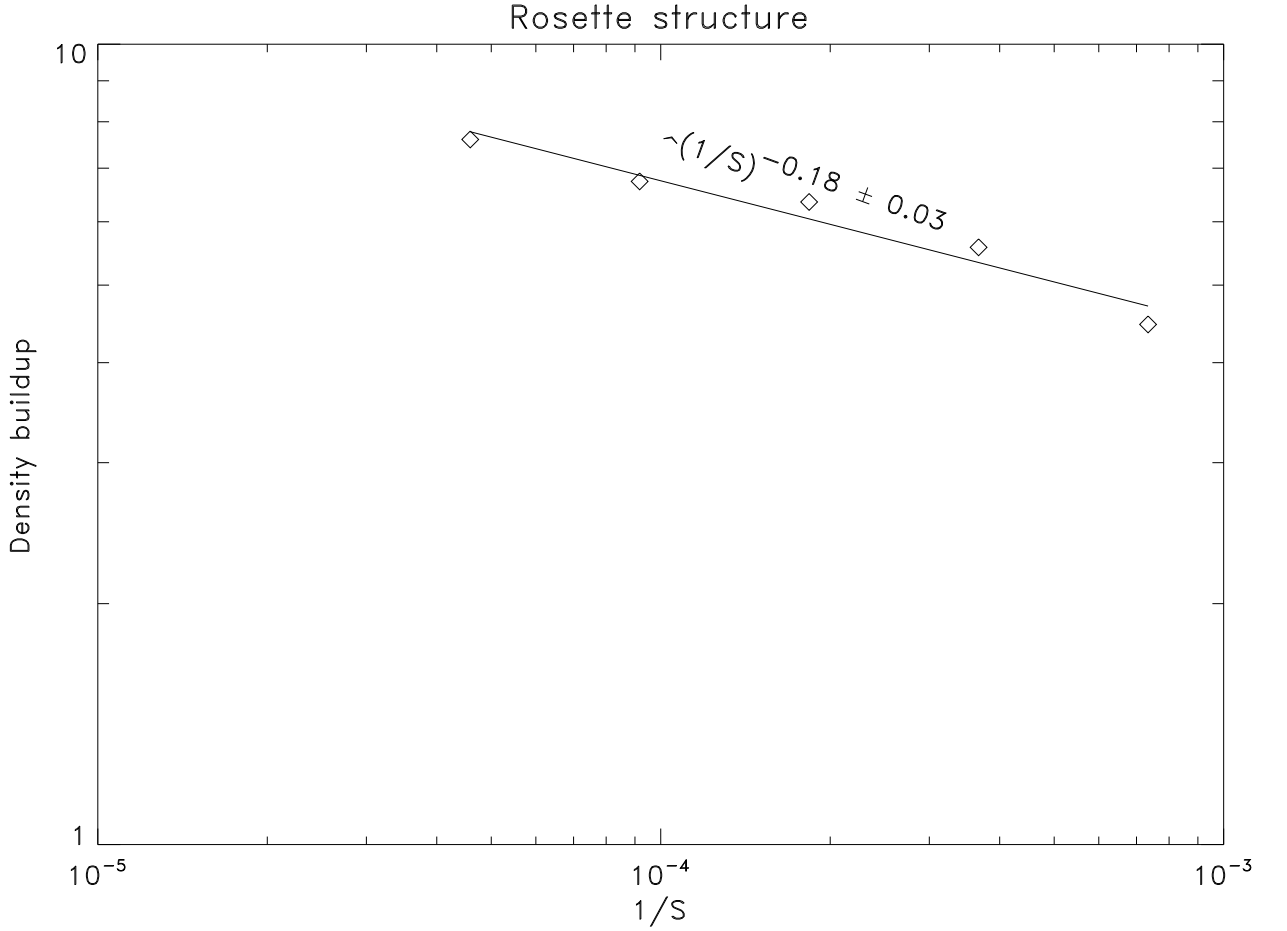


FIG. 6: Density buildup in case of rosette structure. Initial density is unity

times, – in this rough estimate we use initial characteristic values. This means that the density would grow the same way. For previous simulations of rosette-structure, this estimate was $1.2 \div 1.5$, or so, while the real compression proved to be much stronger, see Fig. 6. The mechanism describing further compression after “natural” due to the maximum of the B_z -component was described in Sec. II. In addition, it can be seen from Fig. 6 that the compression grows with decreasing resistivity with some scaling explained in Sec. VIA.

For $Z \gg 1$, the real evolution of the density is defined by the gravity forces, and, as mentioned in Sec. III, is not significant. However, we can calculate the “pseudo-density”, that is, knowing the velocity field from the simulations, we can calculate the density which would be real if the gravity force are switched off. Using Lagrangian solution of the mass

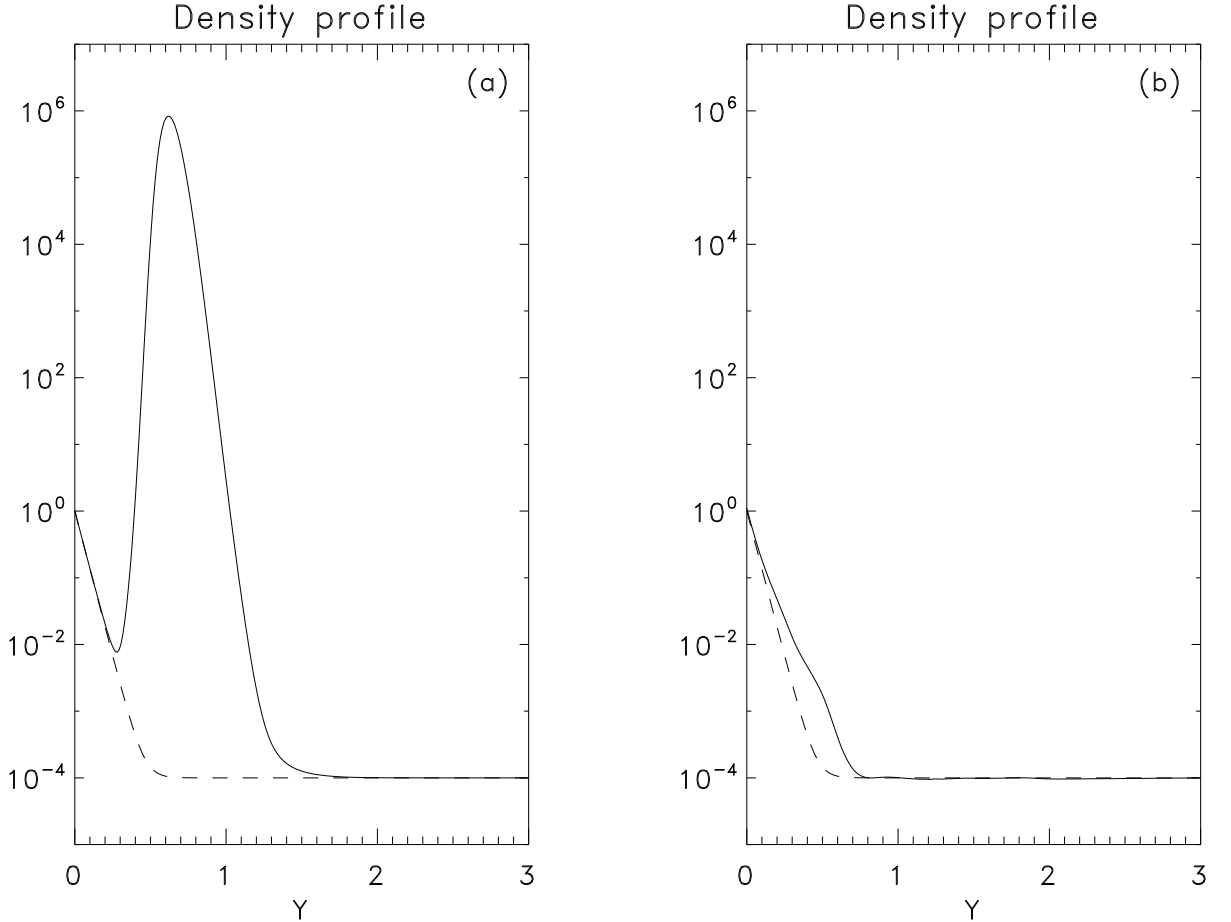


FIG. 7: Density buildup at the Y -axis, depicted by solid lines. Dashed lines correspond to the initial state. For both cases $\eta = 0.00125$, and (a) is for $t = 1$ and $B_{\perp}/B_z = 100$, while (b) corresponds to $t = 5$, and $B_{\perp}/B_z = 2$

conservation equation, we obtain results some examples of which are depicted in Fig. 7.

It is obvious that, for strongly compressible case, depicted in Fig. 7(a), the compression is much stronger than “natural”, that is only 100, while in essentially incompressible case, depicted in Fig. 7(b), the compression is not significant. We note however, that the behavior of “pseudo-density” is only an illustration of strong compression, as opposed to the measurements of the density evolution in previous simulations with $Z = 0$.

VI. RESULTS OF NUMERICAL SIMULATIONS: THE SCALING

A. Ohmic decay and scaling relationships

The process of reconnection is accompanied by Ohmic decay. In regular astrophysical conditions it is quite weak, because the field is frozen-in into the plasma. The situation is different in the presence of current sheets. The energy release during the Ohmic decay is described as follows,

$$\frac{\partial}{\partial t} \int B^2 dx dy = -\eta M = -\eta \int (\nabla \times \mathbf{B})^2 dx dy, \quad (27)$$

or, as an estimate,

$$\frac{1}{t_R} B^2 L^2 \approx \eta \frac{B^2}{\delta^2} \delta L, \quad (28)$$

where on the right-hand-side the volume of the current sheet of the width δ is estimated as δL because, from the numerical experiment, the length of the current sheet does not change much and it is taken to be L .

Then, the estimated reconnection rate,

$$\omega_R = \frac{1}{t_R} = \frac{\eta}{\delta L},$$

or, in dimensionless form,

$$\Omega_R = \frac{t_A}{t_R} = \frac{L}{\delta} \frac{1}{S}. \quad (29)$$

For SP current sheet, δ is defined in (6), and, according to (29),

$$\Omega_{SP} = \frac{1}{S^{1/2}}, \quad (30)$$

cf. (1). Further compression of the sheet width, that is, decreasing of δ , would result in increase of the reconnection rate. In order to estimate this compression, we write (29) in equivalent form,

$$\Omega_R = \frac{L}{\delta_{SP}} \frac{\delta_{SP}}{\delta} \frac{1}{S} = \frac{\delta_{SP}}{\delta} \frac{1}{S^{1/2}},$$

or, the compression can be defined as

$$\frac{\rho}{\rho_0} = \frac{\delta_{SP}}{\delta} = \Omega_R S^{1/2}, \quad (31)$$

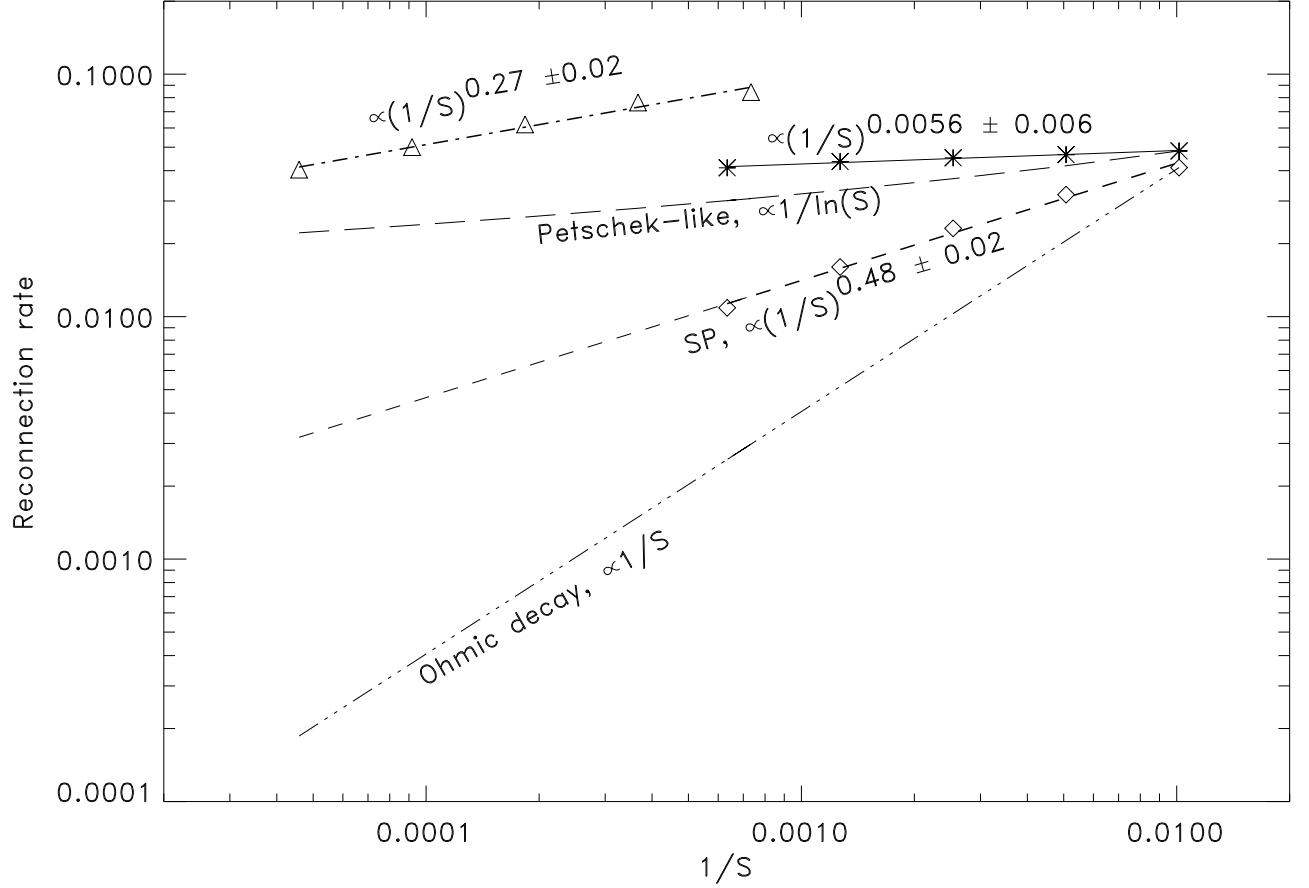


FIG. 8: The reconnection rate, exponents with power-law fitting. Previous runs, $Z = 0$, $\beta = 0.01$, depicted by triangles. Asterisks correspond to $Z \gg 1$, and $B_z/B_\perp = 0.01$. The case of $B_z/B_\perp = 0.4$ and $Z \gg 1$ (diamonds) is essentially incompressible.

where ρ_0 is initial density. This relationship between the reconnection rate and compression will be used below.

Note that direct measurements of the current sheet width δ could be bias. Much more reliable are measurements of integral quantity M defined in (27), the measure of Ohmic decay. According to (27–28),

$$M \approx \frac{B^2 L^2}{t_R \eta} \sim \Omega_R S \quad (32)$$

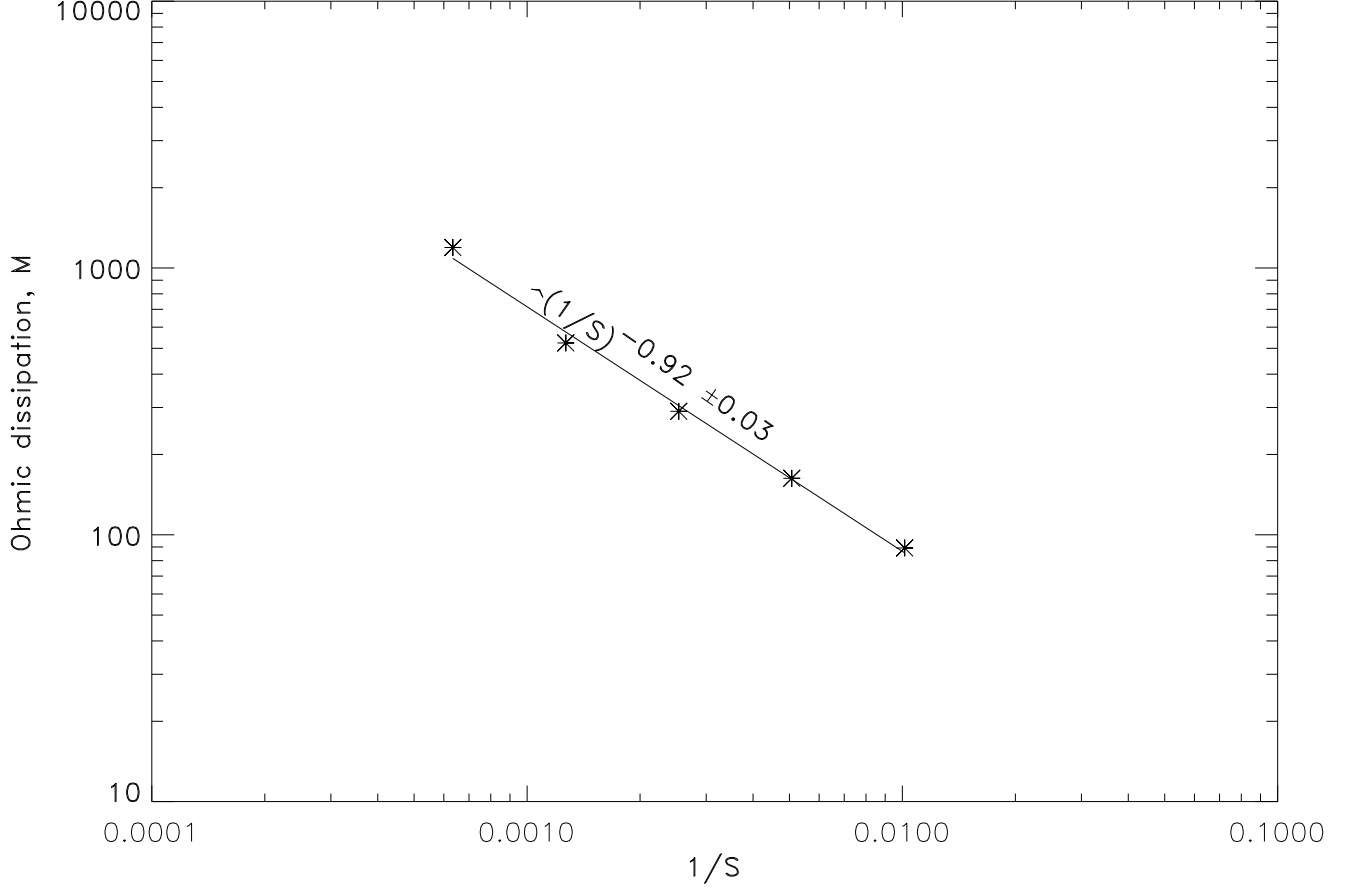


FIG. 9: Ohmic dissipation, M , defined in (27), as a function of Lundquist number S . Here $Z \gg 1$, and $B_z/B_\perp = 0.01$.

B. Scaling laws

Our main results are summarized in Fig. 8. Previous calculations correspond to $Z = 0$, and they definitely show reconnection faster than SP rate. All new simulations correspond to the opposite limiting case $Z \gg 1$. If $B_z/B_\perp = 0.4$ then the velocity proved to be incompressible, and then the SP mechanism is recovered (depicted with diamonds and fitted with short dashed line). On the other hand, if $B_z/B_\perp = 0.01$, the plasma is strongly compressible, as illustrated in Fig. 7. Then, the scaling (fitted with a solid line) is practically flat. Note that the asterisks in the figure correspond to the measurements of averaged electric

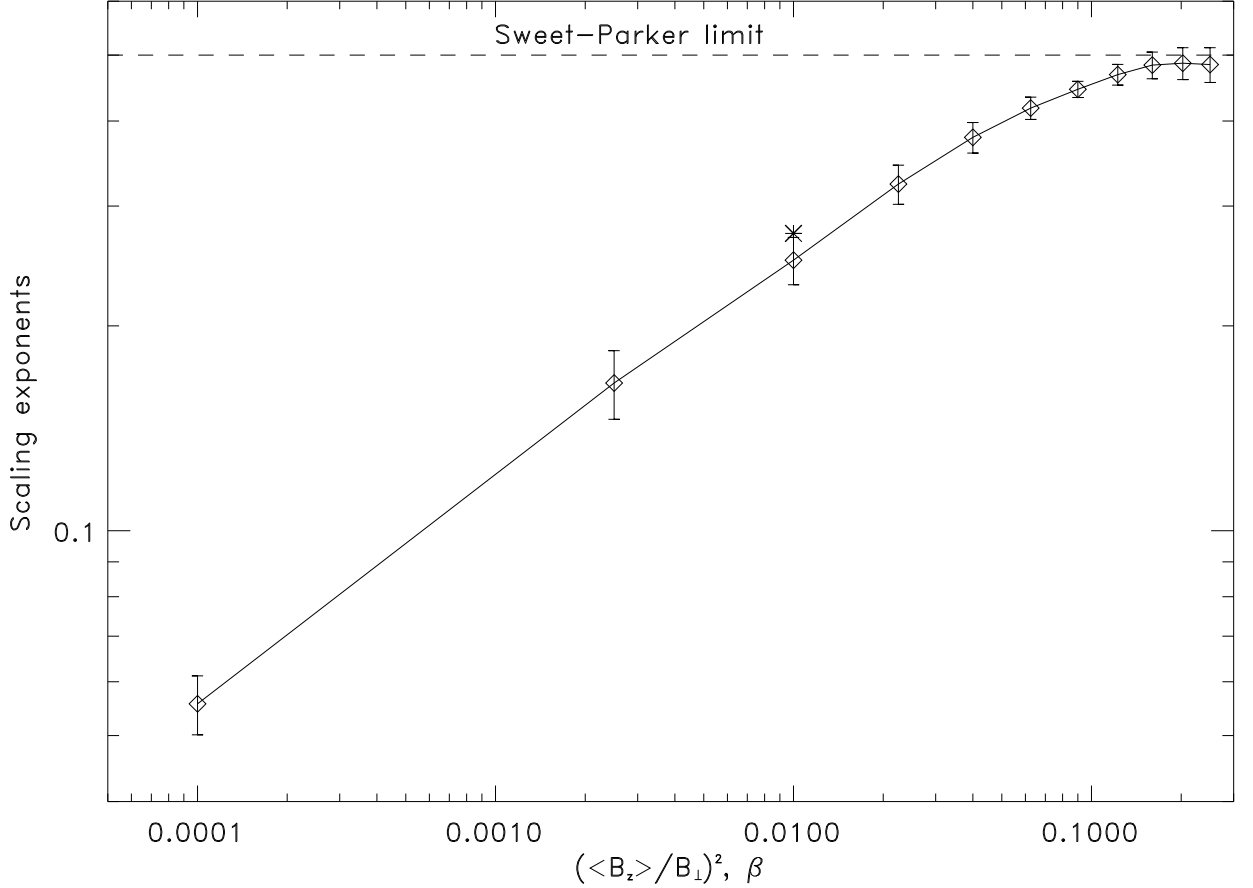


FIG. 10: The scaling exponents depending on compressibility. The diamonds correspond to the different values of $(B_z/B_\perp)^2$, and $Z \gg 1$, while the asterisk corresponds previous simulations, $\beta = 0.01$ and $Z = 0$.

field, see Subsection V A, normalized on maximal electric field, (25). Therefore, the actual numbers should be compared with unity. It can be seen from the Fig. 8 that the numbers are reasonable, not very small.

Another check of the consistency of the theory is the scaling of the density build-up depicted in Fig. 6. According to (31), the compression should scale as $S^{0.23 \pm 0.05}$, which is consistent with the observed scaling given in Fig. 6.

Finally, the scaling of Ohmic dissipation is shown in Fig. 9. This is roughly consistent with predicted in (32), although it does not exactly correspond to it, presumably because

all observed scaling laws can be trusted up to the first decimal number, in spite of the fact that the dispersion of the points is less than that, as can be seen in all figures.

C. Scaling laws as a function of compressibility

We also provided numerical simulation in the same scaling range as in Fig. 8 for different compressible media, while all other initial parameters (like density and magnetic field distribution, etc.) are the same as in all simulations. The compressibility is changing with the parameter $(B_z/B_\perp)^2$. When this parameter is small, then the media is highly compressible, while increasing this parameter, we will approach essentially incompressible situation. As seen from Fig. 10, the incompressible media is reached when $(B_z/B_\perp)^2 = .04$, and then the Sweet-Parker approximation is recovered. For higher compressibility we found that the reconnection is faster (i.e., the scaling exponents are smaller). Note that previously simulations correspond to moderate compressibility, in which case the reconnection is faster than SP mechanism, but still slower than what we have in case of high compressibility.

Acknowledgments

We thank E.N. Parker, B.C. Low, F. Cattaneo and R. Rosner for numerous discussions, and F. Cattaneo and A. Obabko for helping with simulations using pseudo-spectral code. This work was supported by the NSF sponsored Center for Magnetic Self-Organization at the University of Chicago.

-
- [1] P.A. Sweet, in *Electromagnetic Phenomena in Cosmical Physics*, edited by B. Lehnert (Cambridge Press, New York, 1958), p. 123.
- [2] E.N. Parker, *J. Geophys. Res.* **62**, 509 (1957).
- [3] H.E. Petschek, in *AAS-NASA Symposium of the Physics of Solar Flares*, NASA-SP 50, edited W.N. Ness (National Aeronautics and Space Administration, Washington, DC 1964), p. 425.
- [4] D. Biskamp, *Phys. Fluids* **29**, 1520 (1986).
- [5] D. Biskamp, *Magnetic Reconnection in Plasmas* (Cambridge University Press, New York, 2000), p. 239
- [6] B.D. Jemella, M/A. Shay, and J.F. Drake, *Phys. Rev. Letters* **91**, 125002 (2003).
- [7] D. Biskamp and E. Schwarz, *Physics of Plasmas*, **8**, 4729 (2001)
- [8] Z. Mikić, S.I. Vainshtein, J. Linker, and R. Rosner, in preparation.
- [9] E.N. Parker, *Astrophys. J. Supplement* **8**, 177 (1963)
- [10] H. Ji, M. Yamada, S. Hsu, R. Kulsrud, T. Carter, and S. Zaharia, *Phys. Plasmas*, **6**, 1743 (1999).
- [11] B.C. Low, *Phys. Fluids* **25**, 402 (1982).
- [12] S.I. Syrovatsky, *Sov. Phys. JETP* **33**, 933 (1971).
- [13] S.I. Vainshtein, Z. Mikić, R. Rosner, and J. Linker, *Phys. Rev. E*, **62**, 1245 (2000).